

MONITORING NANOPARTICLE AGGREGATION BY COHERENT LIGHT SCATTERING MEASUREMENTS

D. Chicea

Physics Department, University Lucian Blaga of Sibiu, Dr. Ion Ratiu Str. 7-9, Sibiu, 550012, Romania

Abstract

In this work a modified Dynamic Light Scattering particle sizing experiment was conducted to assess the variation in time of the average diameter of the ferrite nanoparticle aggregates in diluted aqueous suspension.

Keywords: nanoparticles, aggregates, Dynamic Light Scattering

1. Introduction

By adding a small amount of nanoparticles in a fluid the heat transfer properties were found to be considerably enhanced [1]. Such a suspension is currently named a nanofluid; it is a relatively new notion and was first mentioned by Choi in 1995 [2].

The nanoparticles have a continuous, irregular motion in nanofluids, which is the effect of several factors such as gravity, Brownian force, Archimede's force and friction force between fluid and the particles. The irregular nanoparticle motion in the fluid is the cause the remarkable enhancement of heat transfer properties of the nanofluids [3-6]. The irregular motion directly depends of the particle dimension therefore the particle size distribution dictates the rheological properties of the nanofluid.

In aqueous suspensions nanoparticles aggregate forming clusters of colloids with an isotropic shape, caused by van der Waals attractions and weak magnetic attractions, which are both of the order of kT [7]. Cobalt nanoparticle are reported to aggregate in "bracelets" [8] which are distinct from the micrometer-sized rings created by rapidly evaporating films of dispersed nanoparticles, with regard to ring size (typically 5-12 particles and 50-100nm in diameter). Reference [9] describes the preparation of robust micrometer size ring structures on mica surfaces. Ring shaped clusters of Co-PFS were patterned onto a thin gold film sputtered

onto a silicon wafer that had been primed with a 5 nm layer of titanium as is reported in [10]. The clusters mentioned in [10] have diameters between 0.6 and 12 μ m.

Nanoparticles are extensively considered for biomedical applications because the living cells have dimensions of the order of microns and parts of the order of tens to hundreds of nanometers. Proteins are even smaller, having dimensions around 5 nanometers. With this in mind, it was easy to imagine that nanoparticle structured materials can be used in many ways to investigate, to modify living cells or to deliver certain substances or drugs to them without perturbing much the cells. Thus many practical applications were developed in the last years and are nicely presented in [11, 12] and in many other review papers, not cited here.

The size and size distribution are crucial in some cases, for example if penetration through a pore structure of a cellular membrane is required. Fe₃O₄ nanoparticles are of special interest for biomedical applications because they are not toxic and they can be metabolized by living organisms. They present a major inconvenient though, as they aggregate very fast in diluted aqueous suspension. As the human body fluids are aqueous solutions, transporting Fe₃O₄ nanoparticles through human blood to a tumor or to a specific organ using magnetic field might create serious problems as the nanoparticles aggregate during the transportation process through the blood vessels. Once big aggregates are present the rheological properties of the suspension are different and the suspension ceases to be a nanofluid any more.

The most accurate and also the most expensive technique used to obtain a very high resolution image of an emulsion containing nanoparticles is the Transmission Electron Microscopy (TEM). An example of using TEM is [13] but other hundreds of papers can be cited to have successfully used the technique in characterizing the nanoparticle size distribution.

Other currently used methods for nanoparticle sizing are Atomic Force Microscopy (AFM), and ferromagnetic resonance (FMR), for magnetic nanoparticles. A comparison of the TEM with the AFM results is presented in [14]. The results in [13] reveal that the AFM measured nanoparticle diameter appears to be reduced with 20% and the standard deviation appears to be increased with 15%. The AFM technique, as the TEM, requires expensive equipment and a delicate, time consuming procedure to prepare the sample.

A lower cost alternative to these techniques and others not mentioned in this introductory part is based on the fact that the nanoparticles have a continuous, irregular motion in nanofluids, which is the effect of several factors such as Brownian force, Archimede's force, friction force between fluid and the particles and gravity, which becomes significant for micron sized particles but can be neglected for nanometer sized particles [15].

The method is called Dynamic Light Scattering (DLS) or Photon Correlation Spectroscopy (PCS) and the physical principles of the method are explained in [16, 17] and other papers following them. Details on a modified version of DLS are presented in the next section, followed by the results on monitoring the aggregates dimension variation in time during a dilution process.

2. Method and sample

Dynamic light scattering (DLS) is a well established technique for measuring particle size over a size range from nanometers to microns. As previously stated the light scattered by a suspension presents fluctuations [12, 16]. By placing a detector at a certain angle and recording the scattered light intensity a time series is produced. As proved in [18, 19] the width of the autocorrelation function of the time series is proportional to the diffusion coefficient, which, on its turn, depends of the particle diameter. This leads to a fast procedure for measuring the particle diameter. An improved version is described further on in this section.

The early experimental works [20, 21] proved the assumption that the power-spectrum of the intensity of the light scattered by particles in suspension can be linked to the probability density function (hereafter PDF). This link between the PDF and the power-spectrum is a consequence of the translation of the relative motion of the scattering particles into phase differences of the scattered light. The phase correlations lead to fluctuations in the intensity of the scattered light recorded using a detector and a data acquisition system, in a typical experimental setup, as presented in Fig. 1.

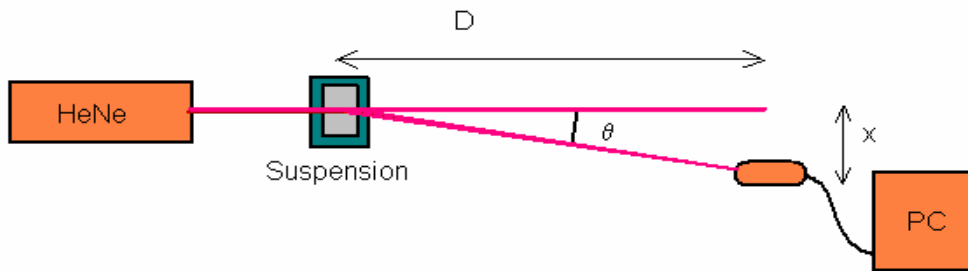


FIGURE 1. A typical DLS experimental setup

By subtracting the average intensity from the recorded time series and calculating the square of the intensity we obtain the power time series. The Fourier transform of the power time series is the power spectrum. We can compare the spectrum calculated from the

experimental data with the theoretically expected spectrum, namely the functional form of the Lorentzian line $S(f)$:

$$S(f) = a_0 \cdot \frac{a_1}{(2\pi f)^2 + a_1^2} \quad (1)$$

The Lorentzian line $S(f)$ has two free parameters a_0 and a_1 and is fit to the power-spectrum using a non-linear minimization procedure to minimize the distance between the data-set and the line. The possibility to fit the whole function is advantageous compared to the alternative method described in [20, 21], where the $f_{1/2}$ (the frequency where half-maximal-height is reached) was measured, since it takes more data points into account, thus increasing the quality of the fit. Once the fit is completed, the diameter of the SCs can be assessed as the double of the radius R . The radius can be derived as a function of the fitted parameter a_1 and other known quantities using (2):

$$R = \frac{2k_B T K^2}{6\pi\eta a_1} \quad K = \frac{4\pi n}{\lambda} \cdot \sin\left(\frac{\theta}{2}\right) \quad (2)$$

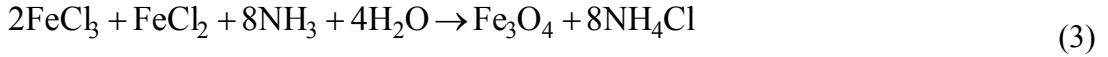
In (2) k_B is Boltzman's constant, T is the absolute temperature of the sample, η is the dynamic viscosity of the solvent, θ is the scattering angle, n is the refractive index of the scattering particles and λ is the wavelength of the laser radiation in vacuum.

The wavelength was 633nm, the light source was a He-Ne laser and the power was 2mW. The DLS experiment was carried on at 20°C. The cuvette-detector distance D was 0.615m and x was 0.03m making the scattering angle θ equal to 2°47'34''. This is not typical for DLS experiment where a bigger angle is chosen, usually 90°. The reason for choosing such a small angle is to shift the rollover point in the Lorentzian line towards smaller a_1 values, hence smaller frequencies, where the noise is considerably smaller.

Prior to the experiment the concentrated nanoparticle suspension was diluted in 25% citric acid, in order to prevent aggregation and a DLS time series was recorded. The time series was analyzed using the procedure described above. The PSD (smooth line) and the fitted Lorentzian (the scattered line) for the time series recorded on sample 1m9-3 are presented in Fig. 2. The parameters of the Lorentzian line found from the fit are: $a_0=2.27$ and $a_1=30.00$. Using (2) we found that the nanoparticles have an average diameter of 18nm.

The nanofluid preparation does not require any special equipment and was carried on at room temperature, which was 22°C. The reagents used were: $\text{FeCl}_3 \cdot 6\text{H}_2\text{O}$, $\text{FeCl}_2 \cdot 4\text{H}_2\text{O}$, ammonium hydroxide ($\text{NH}_3[\text{aq}]$) 25%, citric acid ($\text{C}_6\text{H}_8\text{O}_7$). A common coprecipitation synthesis method was followed and was carried on at room temperature. The surfactant was

citric acid. The recipe and the procedure for manufacturing the nanofluid are presented in detail in [22]. Overall, the chemical reaction that produced the nanoparticles was:



The volume ratio was 33%.

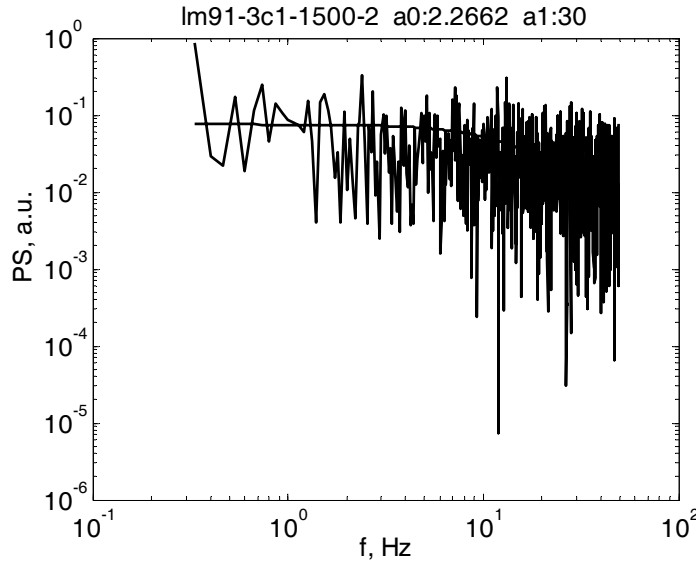


FIGURE 2. The PSD (scattered line) and the fitted Lorentzian function (smooth line) for the time series recorded on sample lm9-3 diluted in citric acid.

3. Results and discussions

First 0.01ml concentrated nanofluid was introduced into a 5ml syringe and after it 4.99ml of deionised water was aspired in. At the time of deionised water aspiration the time series recording was started. The mixture was injected fast into the cuvette producing turbulences. Right after that a certain fluid quantity was aspired and injected back. The procedure of aspiring and injecting fast the suspension was repeated three times in order to obtain a homogeneous suspension. The amount of aspired fluid was small enough that the laser beam remained under the upper surface of the fluid at all times. Anyway, due to the turbulences produced by the aspiration procedure the velocity of the SCs was different from the velocity of the natural Brownian motion and this can lead to false DLS particle size. For this reason the first 7 seconds from the first slice of the time series was not processed as previously described.

A 900 seconds time series was recorded using the values of the parameters describes above. As the purpose of the experiment was to monitor the nanoparticle aggregation process, a program was used to slice the time series into chunks of data, using the desired time interval

for each data chunk or slice, which is given as an input parameter. We should note however that using a small time span for each data slice will apparently increase the accuracy of the monitoring process but will decrease the precision of the Lorentzian function (1) fit as the amount of data to be fitted is smaller. Increasing the time span for each data slice will increase the precision of the fit, but will provide a poor information of the variation of the aggregates dimension in time. With this in mind, the time span of each time series slice was chosen to be 15 seconds.

Special care must be taken to start the recording simultaneously with the beginning of the dilution process and to produce a strong agitation and stirring of the aqueous suspension, otherwise the diffusion of the nanoparticles is slow compared with the time span of the experiment and the results might not be reproducible as different concentrations might occur in the beam area of the cuvette.

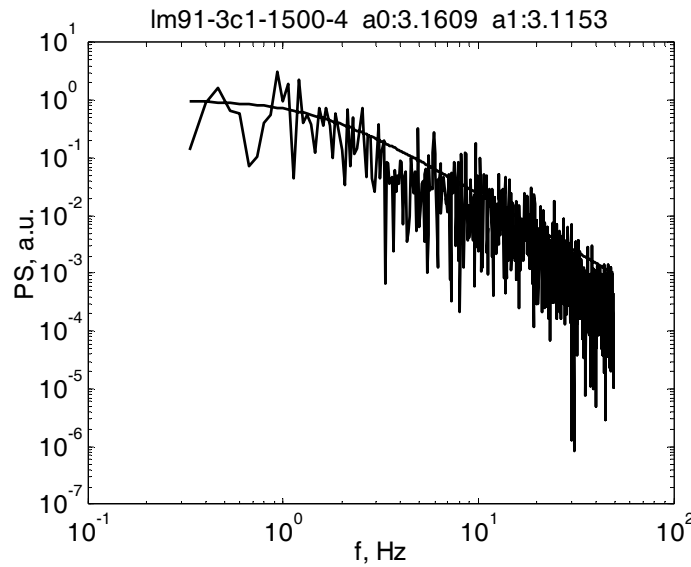


FIGURE 3. The PSD (scattered line) and the fitted Lorentzian (smooth line) for the time series slice allotted to time 11s since the dilution was started on sample lm9-3.

The PSD (blue line) and the fitted Lorentzian line for the first time series, allotted to time 7+4=11s are presented in Fig. 3. The parameters of the Lorentzian line that produce the best fit are: $a_0=5.0034$ and $a_1=1.2615$. Using (3) we found that the particles have an average diameter of 418nm, considerably bigger than the average diameter of the SCs measured in the concentrated suspension.

The fitting procedure was repeated for all the consecutive time slices recorded during the experiment and the average diameter was calculated. The variation of the average

diameter in time calculated using the modified version of the DLS particle sizing, as described above, is presented in Fig. 4.

We should notice, however, that the diameter we measured using the procedure described above, which is basically a DLS using nontypical values for the experimental parameters and for the detection system, is the hydrodynamic diameter, which is slightly different from the physical diameter. Moreover, the presence of particles with a wide diameter distribution changes the shape of the PSD departing it from the theoretical shape, as presented in Fig. 3.

Examining Fig. 4 we notice a very fast increase of the average aggregate diameter in time. Actually after 22.5 seconds since the dilution was initiated we can no longer consider nanoparticles in suspension as the average measured diameter was bigger than $1\mu\text{m}$. As time passed the average diameter increasing rate decreased and a plateau can be noticed after 40 seconds. The average aggregate diameter remained around $1\mu\text{m}$; the variation around the average plateau value might be an artifact of the fitting procedure.

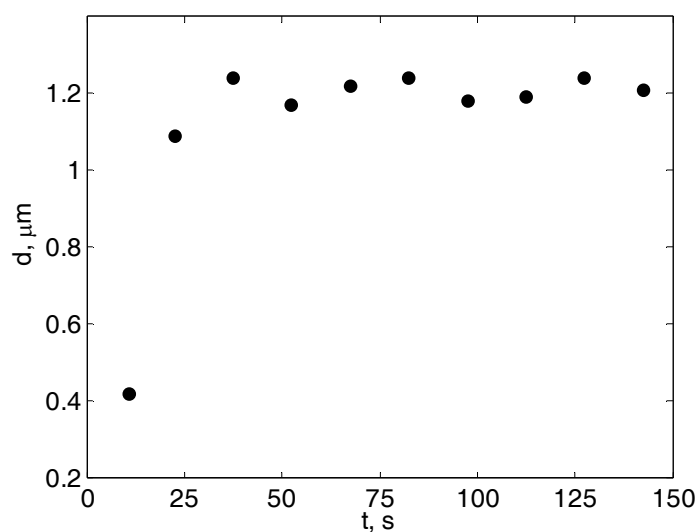


FIGURE 4. The variation of the nanoparticle aggregates average diameter in time.

Conclusions

In this work a simple experimental procedure, assisted by a set of computer programs required to process the data is presented. Using this procedure we found that magnetite nanoparticles having citric acid as surfactant, in aqueous diluted suspension, 0.07% volume ratio, aggregate very fast. During the first 20 seconds the aggregates dimension increases and the size reached a diameter bigger than $1.0\mu\text{m}$ and this is extremely important when considering the nanoparticles for biomedical applications.

References

1. P. Vadasz, J. Heat Transfer. 128 (2006) 465.
2. U. S. Choi, ASME Fed. 231 (1995) 99.
3. S. P. Jang and S. U. S. Choi, Appl. Phys. Lett. 84 (2004) 4316.
4. W. Evans, J. Fish and P. Keblinski, Appl. Phys. Lett. 88 (2006) 093116.
5. Y. M. Xuan and W. Roetzel, Int. J. Heat Mass Transfer. 43 (2000) 3701.
6. R. Prasher, P. Brattacharya and P. E. Phelan, Phys. Rev. Lett. 94 (2005) 025901.
7. K. Butter, P. H. Bomans, P.M.Frederik, G. J. Vroege and A. P. Philipse, J. Phys.: Condens. Matter 15 (2003) S1451, doi: 10.1088/0953-8984/15/15/310.
8. S. L. Tripp, S. V. Pusztay, A. E. Ribbe, A. Wei, J. Am. Chem. Soc. 124 (2002) 7914.
9. Z. Xiao, C Cai, X. Deng, Chem. Commun., (2001) 1442, doi: 10.1039/b104306b.
10. S. B. Clendenning, S. F. Bidoz, A. Pietrangelo, G. Yang, S. Han, P. M. Brodersen, C. M. Yip, Z Lu, G. A. Ozin, I. Manners, J. Mater. Chem., 14 (2004) 1686.
11. O. V. Salata, Journal of Nanobiotechnology 2 (2004) 3, doi:10.1186/1477-3155-2-3.
12. J. David Briers, Physiol. Meas. 22 (2001) R35.
13. F. Zhang, S.W. Chan, J. E. Spanier, E. Apak, Q. Jin, R. D. Robinson, I. P. Herman, Appl. Phys. Lett. 80 (2002) 27; doi:10.1063/1.1430502.
14. L. M. Lacava, B. M. Lacava, R. B. Azevedo, Z. G. M. Lacava, N. Buske, A. L. Tronconi and P. C. Morais, Journal of Magnetism and Magnetic Materials, 225, 1-2 (2001) 79.
15. D. Chicea, Applied Optics, 47, 10 (2008) 1434.
16. J.W. Goodman, Laser speckle and related phenomena, Vol.9 in series Topics in Applied Physics, J.C. Dainty, Ed., Springer-Verlag, Berlin, Heidelberg, New York, Tokyo, (1984).
17. M. Giglio, M. Carpineti, A. Vailati and D. Brogioli, Appl. Opt. 40 (2001) 4036.
18. W. Tscharnuter, in Encyclopedia of Analytical Chemistry, R.A. Meyers (ed), John Wiley & Sons Ltd, (2000), 5469.
19. B. B. Weiner, Chapt. 5 in Liquid-and Surface-Borne Particle Measurement Handbook, J. Z. Knapp, T. A. Barber and A. Liebermann (ed), Marcel Dekker Inc. NY, (1996).
20. N. A. Clark, Lunacek JH, Benedek GB, American Journal of Physics, 38, 5 (1970), 575.
21. S. B. Dubin, Lunacek JH, Benedek GB, PNAS, 57(5) (1967) 1164.
22. D. Chicea, C. M. Goncea, Optoelectronics and Advanced Materials – Rapid Communications 3 (2009) 185.